Lawrence Berkeley National Laboratory

Title

Radiation Problems in the Design of a Radioactive Nuclear Beam Facility

Permalink

https://escholarship.org/uc/item/185715vm

Authors

Donahue, R J
Nitschke, J M
Stoyer, M A
et al.

Publication Date

1994-04-01

Lawrence Berkeley Laboratory
UNIVERSITY OF CALIFORNIA

ENVIRONMENT, HEALTH AND SAFETY DIVISION

**Radiation Problems in the Design of a Radioactive
Nuclear Beam Facility**

R.J. Donahue, J.M. Nitschke, M.A. Stoyer, and G.C. Moeller

April 1994

DISCLAIMER

Radiation Problems in the Design of a Radioactive Nuclear Beam Facility

R. J. Donahue, J. M. Nitschke, M. A. Stoyer

Lawrence Berkeley Laboratory
Berkeley, CA 94720

G. C. Moeller

University of California, Berkeley
Berkeley, CA 94720

ABSTRACT

Radioactive Nuclear Beam (RNB) facilities are proposed or under construction in North America, Japan, Russia, and in Europe. The front ends of these facilities are very similar to intense neutron spallation sources in that they require approximately 1 GeV, ≥ 100 μA proton beams incident on thick high-Z targets, possibly including enriched uranium. This paper will summarize some of the radiation transport modelling problems and solutions encountered in the preconceptual design of such a facility. Issues to be addressed include Monte Carlo and discrete ordinates modelling of deep penetration shielding, target heating and residual mass yields. Comparisons are made between empirical data (Tsao and Silberberg), when available, and computer codes (FLUKA, LAHET, TWODANT). Suggestions are made for further improvement and development of existing models and experimental measurements.

1. Introduction

Numerous conferences and workshops have drawn attention to the science and technical aspects of radioactive nuclear beam facilities [1-5]. There are current plans [6] for such facilities, in North America [7], Japan, Russia, and in Europe [8]. The rapidly expanding field of Radioactive Nuclear Beam (RNB) research offers the promise of new horizons in such fields as nuclear structure, low-energy nuclear reactions, astrophysics, atomic physics and materials science. Proposed future RNB facilities will be extremely flexible and capable of producing intense RNB's ranging in mass from very light elements up to and including uranium.

Recent work at LBL has centered around the ISOL (Isotope Separator On-Line) approach to producing RNB's [9]. The conceptual plan details a primary accelerator directing proton beams of 100-200 μA and 500 to 1000 MeV energy onto a variety of thick targets. In this respect, the IsoSpin Laboratory (ISL) will have many radiation-related challenges in common with current and planned neutron spallation sources. However, several challenges are unique to the ISL. For example, it is important in the design of the optimum target to accurately predict the yields of radioactive isotopes which may be far from stability. It will also be very important to determine heating profiles in the target to be able to prevent radioactive species from condensing out in target cold pockets or structural failure of the target due to overheating. The crucial difference between a neutron spallation source and an ISL target is that the latter is <u>open</u>, *i.e.*, it is designed to release radioactive products with the highest possible efficiency. This paper summarizes ongoing work in three different areas: deep penetration shielding necessitated by the high current primary proton beam, calculation of target radioactive inventories and target heating.

2. Radiation Shielding

The high primary proton beam current (100-200 μA) combined with ever-decreasing dose rate criteria (100 mrem/2000 hr-yr at LBL) requires ISL shielding to provide attenuation factors on the order of 10^{10}. This presents a serious modelling problem, since to transport one high-energy neutron through the shield would require following on the order of 10^{10} histories, assuming each incident 1 GeV proton creates on the average one high-energy neutron. Such simulations are unrealistic even using today's supercomputers with unbiased Monte Carlo codes. There are well known methods for estimating bulk shielding at large angles in these energy ranges [10]; however, these methods understandably fail at small angles and for relatively thin shields. Our goal was to be able to estimate bulk shield thicknesses in the forward, as well as the lateral directions, and to be able to predict doses at relatively close distances to the target. The doses were used to provide radiation damage estimates for ISL components which must be in close proximity to the targets.

The solution employed was to couple the output of the LAHET Monte Carlo code [11], after sufficient transport (see below) through the shield, to the ONEDANT [12] discrete ordinates code for subsequent transport. The neutron multigroup cross-section set, HILO(R1) [13], is used for the ONEDANT analyses. This cross-section set has an upper neutron energy limit of 400 MeV. A possible solution for modelling neutrons created above 400 MeV is to place them in the last HILO(R1) group and weigh them by the ratio of their real energy to the energy of the last HILO(R1) consistent with energy conservation. For example, a 700 MeV neutron would be placed in the highest HILO(R1) group (375-400 MeV) and its weight would be increased to 1.81. Rather than introduce the uncertainty associated with this ratio, the LAHET calculations were continued to a depth where contributions from neutrons with energy greater than 400 MeV is negligible. The LAHET output is then used as the input to the ONEDANT analyses. The thickness of ordinary concrete necessary to satisfy the approximation of neglecting neutrons with energies above 400 MeV was determined to be about 2 meters.

The neutron spectra at 0° at various depths in the concrete shield from a 1 GeV proton beam incident on a tantalum target are shown in Fig. 2.1. Target thickness is equal to the range of a 1 GeV proton in tantalum. The distance from the target to the concrete shielding is 1 m in all directions.
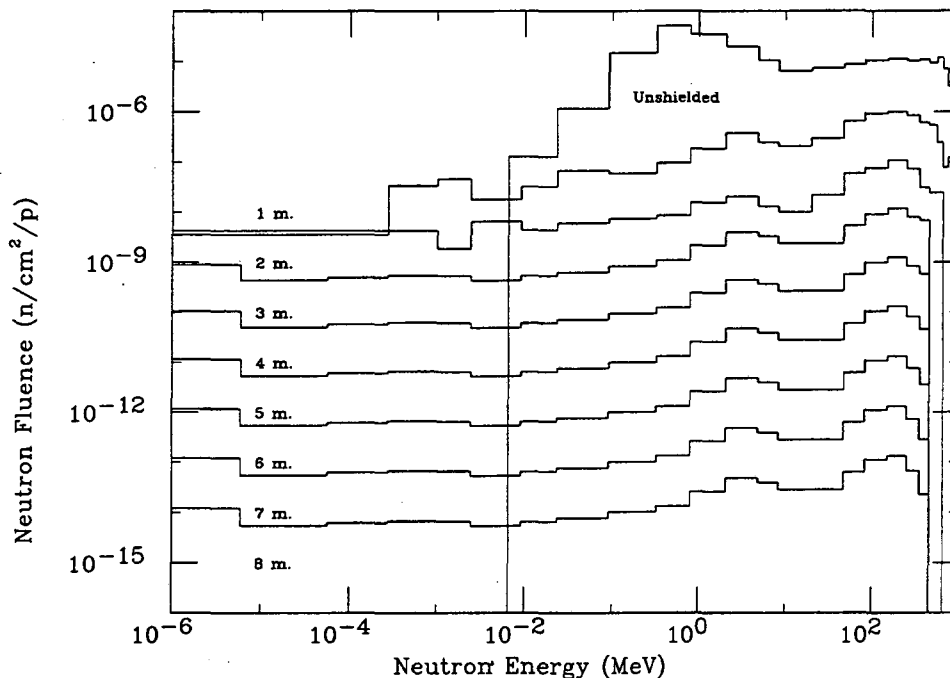
Figure 2.1: Neutron fluence vs. neutron energy at 0° at various concrete thicknesses for 1 GeV protons on a thick Ta target. LAHET/ONEDANT coupling occurs at 2 meters of concrete. Neutron fluence has been normalized by the log of the energy bin width. The distance from target to shield is 1 m.

The nuclear interaction length in concrete, λ_I, is taken as 42 cm [14]. One can see from Fig. 2.1 that an equilibrium spectrum of neutrons is obtained after a penetration of $\sim 5\lambda_I$. At this thickness, only relative attenuation in the spectra occurs in the few highest energy groups with all other energy groups in relative equilibrium.

The dose rate at 0° and 90° as a function of concrete thickness is shown in Fig. 2.2. Dose conversion factors are taken from Belogorlov [15].

Fig. 2.3 shows the dose attenuation mean free path for thick concrete shields at 0° and 90° to the incident proton beam along with the high energy limiting value by Tesch [10]. The dose attenuation mean free paths after 7 meters of concrete are approximately 100 g/cm^2 and 94 g/cm^2 at 0° and 90°, respectively. LAHET results are plotted from 0 to 2 meters and TWODANT results are plotted from 2 to 8 meters. LAHET analyses were carried out to 3 meters to compare with the TWODANT results between 2 and 3 meters
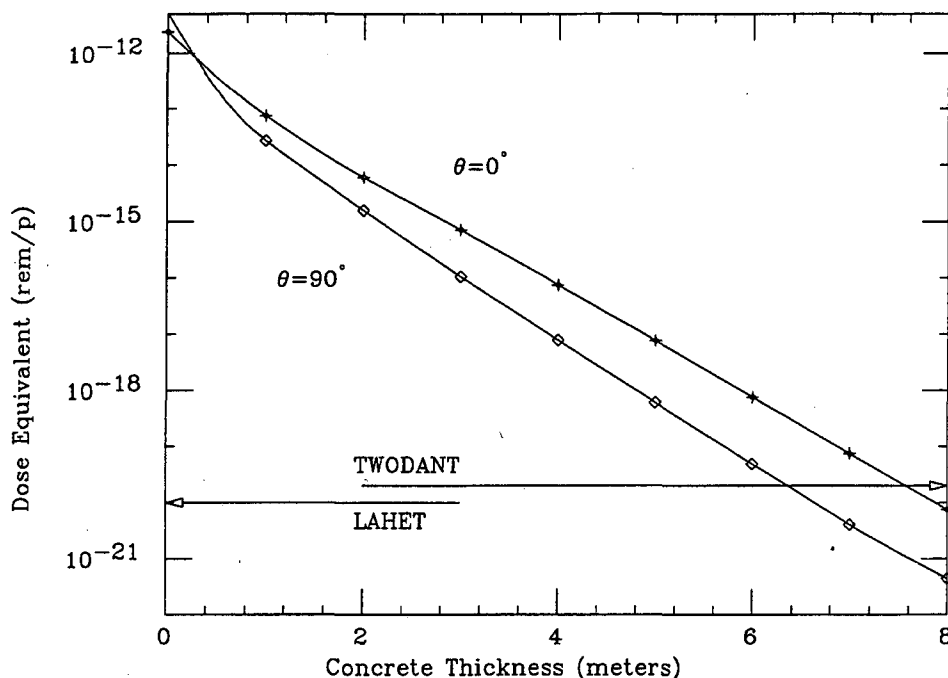
Figure 2.2: Neutron dose equivalent vs. concrete thickness at 0° and 90° for 1 GeV protons on a thick Ta target. The distance from target to shield is 1 m.

and the results are indistinguishable. It should be noted that dose equivalent rates close to the target and at large angles are highly dependent upon the target geometry.

Several parameters were varied in order to study the sensitivity on of the results, including; LAHET neutron cutoff energy and ONEDANT order of angular quadrature. None of these parameters had a significant effect on the overall dose results. Of particular interest was the fact that the neutron energy cutoff from LAHET at 2 meters into the concrete could be raised as high as 10-20 MeV, and following an additional 1 meter of transport by ONEDANT, the equilibrium spectrum had re-established itself as previously determined with much lower LAHET cutoff energies.
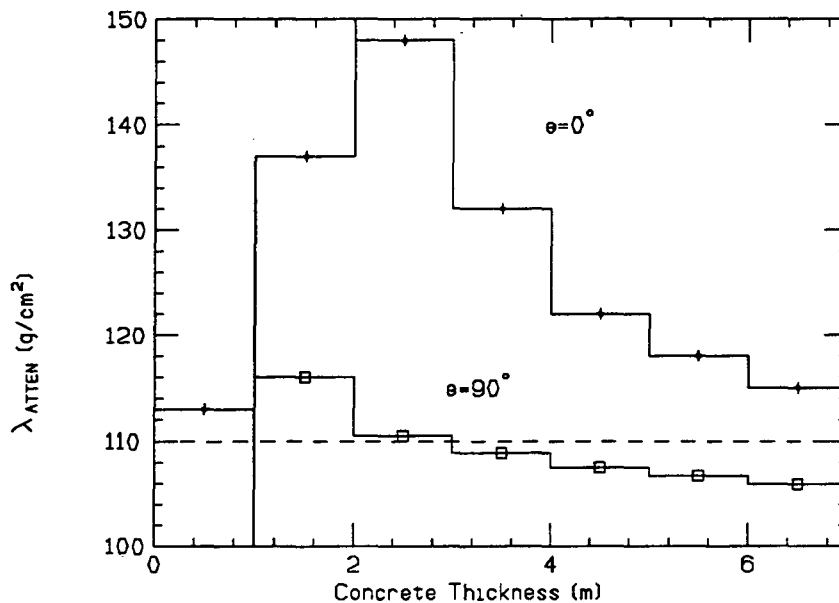
Figure 2.3: Neutron attenuation mean free path vs. concrete thickness at 0° and 90° at various concrete thicknesses for 1 GeV protons on a thick Ta target. The high energy limit of 110 g/cm² is taken from Tesch [10].

3. Isotope Yields

The prediction of products in various targets is essential to any RNB facility. The CERN ISOLDE facility has published [16] measured intensities of many radioactive beams, however, these measurements involve several unknown factors in trying to relate these results to target yields such as decay due to target holdup time and ionization and acceleration efficiencies. It is important to predict target yields not only because it is necessary to predict the intensities of radioactive beams that can be delivered for experiments but also from a safety/hazard point of view.

The importance of beam intensity estimates for experimenters is obvious. The majority of the experiments at RNB facilities are beam intensity limited. Uncertainties in yields of factors of 10 are common and are the difference between an experiment requiring 1 or 10 weeks of beam time. This is a significant factor in determining whether an experiment is feasible.

The safety concern is not just activation analyses for the purposes of determining residual dose rates, since this will clearly require remotely handled operation at the facility [17], but the requirement for more detailed isotope production analyses. A recent DOE Order [18] determines the categorization, and hence the design, as a non-reactor nuclear facility based "only on the quantities of radioactive materials in the facility." The DOE Order has an appendix which lists, by isotope, threshold quantities for various categories of the non-reactor nuclear facility classification. This DOE Order was written to allow a graded approach in preparing the Safety Analysis Report of any facility, but it is unclear whether such a graded approach can be used in the actual design and construction of a non-reactor nuclear facility. The impact of having to meet many of the nuclear facility standards is likely to be significant and costly. Spallation, fission, fragmentation, and to some extent peripheral reactions are the processes for radioactive isotope production by medium-energy proton beams incident on ISL targets. Spallation products are produced over the entire range on nuclides but tend to be produced closer to the mass of the target nucleus, with a corresponding buildup of low-mass fragments, and generally on the proton rich side of the valley of stability because of the large multiplicity of evaporation neutrons. Fission mass yields are highly dependent on the energy of the particle inducing fission. Low-energy fission processes produce mass yield curves which resemble bivariate gaussian distributions and are peaked in the mass ranges of ~90-100 and ~130-140 for a ^{235}U nucleus. Fast fission ($\geq$20 MeV) mass yields are more symmetric with equal probability of producing fragments with masses between ~90 and ~140. Fission products are also preferentially produced on the neutron rich side of the valley of stability. Fission is dominant in high-Z targets like UC and ThC, but is also important in other heavy targets such as Pb and Bi. The net result is an efficient means of producing RNB's on both sides of the valley of β-stability and for all masses.

An example of the isotopic intensities produced by a 600 MeV, 100 μA proton beam incident on a 1 mole/cm^2 thick UC target is shown in Fig. 3.1. These yields were obtained using a computer code that is based on the work of Silberberg and Tsao (see [19] and references therein).

The Silberberg and Tsao predictions are based on a compilation of experimental data combined with semi-empirical extrapolations in regions where data was not available and do not include radioactive decay losses, secondary reactions, and feeding from radioactive

Radioactive Beam Intensities

(1 GeV Protons, 100 μA, on 56g/cm^2 CaO)
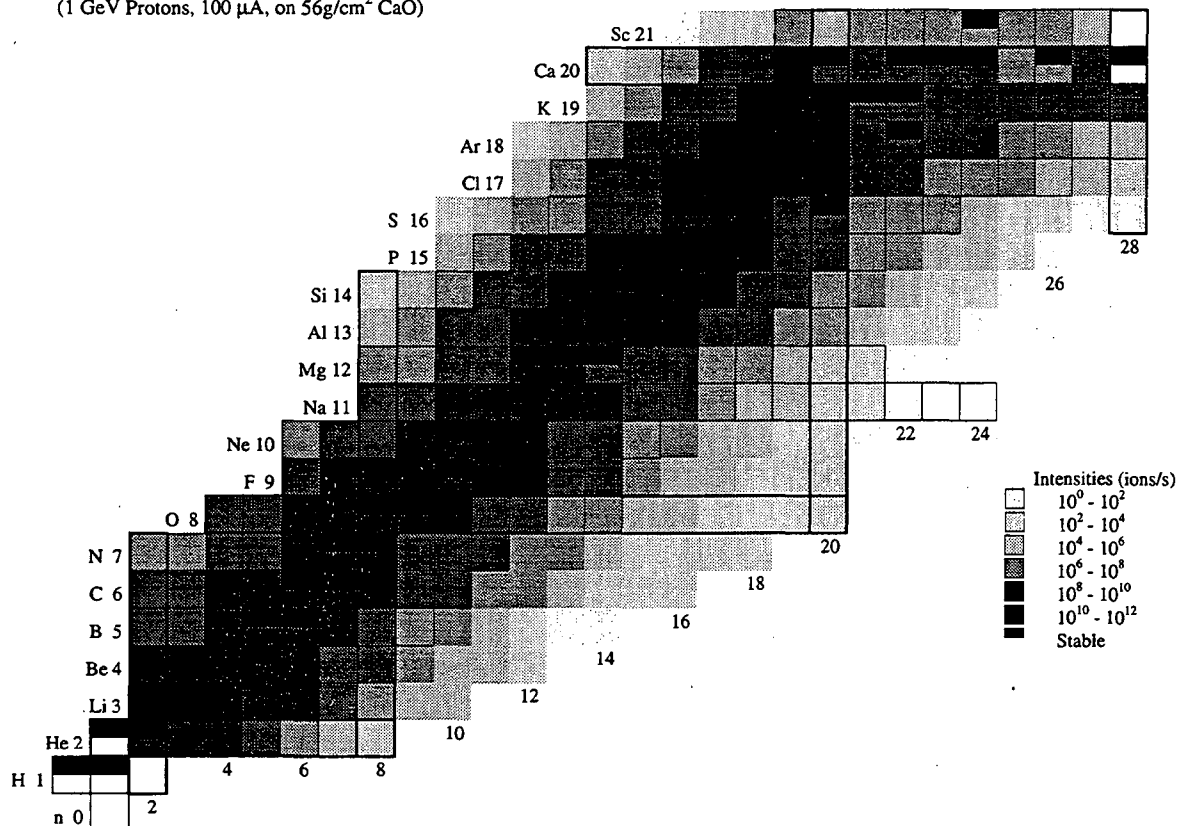
Figure 3.1: Example of isotope intensities produced by a 600 MeV 100 μA proton beam incident on a 1 mole/cm^2 thick CaO target. This figure is available via anonymous ftp at InterNet node 128.3.12.48 in color PostScript format in /pub/ISL.

decays. To properly predict isotopic yields, several computer programs have been developed. A block diagram denoting these programs is shown in Fig. 3.2. Dashed lines indicate missing programs or missing connections between programs. The LAHET Monte Carlo program has been discussed previously and transports neutrons to 20 MeV. The MCNP program handles the transport of neutrons below 20 MeV and gives neutron fluxes (Φ). The TSAO program gives predicted yields based on experimental data and extrapolation ("Semi-empirical"). "High" mass yields are the residual mass distributions given by LA-HET which don't include contributions from neutrons with energies lower than 20 MeV.
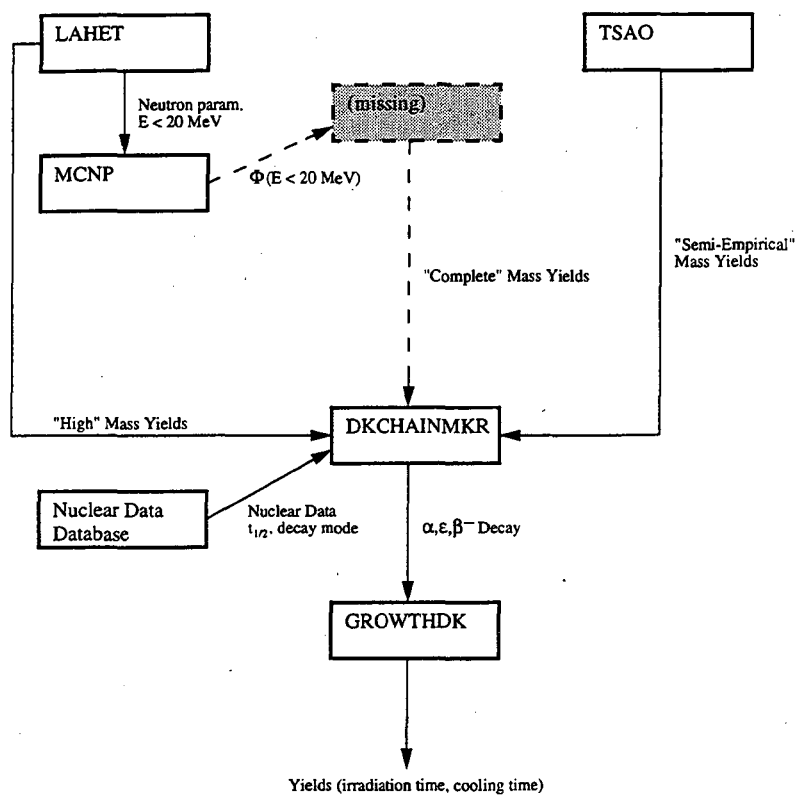
Figure 3.2: Schematic representation of programs for calculation of isotopic yields. The symbols and abbreviations are defined in the text.

"Complete" mass yields (including all neutrons) are currently not available. The program DKCHAINMKR extracts nuclear data from a database (half-life, $t_{\frac{1}{2}}$; decay mode; branching ratios; etc.) and constructs decay chains, including alpha decay (α), electron capture (ϵ), and beta-decay (β^-). The final program, GROWTHDK, calculates the growth and decay of each isotope not only during proton beam irradiation of the target, but also during "cooling" times and gives calculated yields as a function of time.

Ideally one would like to be able to take the predicted residual mass yields from a radiation transport code, like LAHET [11] or FLUKA92 [20] and use this as input to a code system for buildup and decay calculations. However, there are several problems with this method. First, simple buildup and decay calculations based on LAHET spallation and fission residual masses do not include isotopes produced by neutron processes below 20 MeV. This may be adequate for medium and low Z materials but is not acceptable for high Z materials.
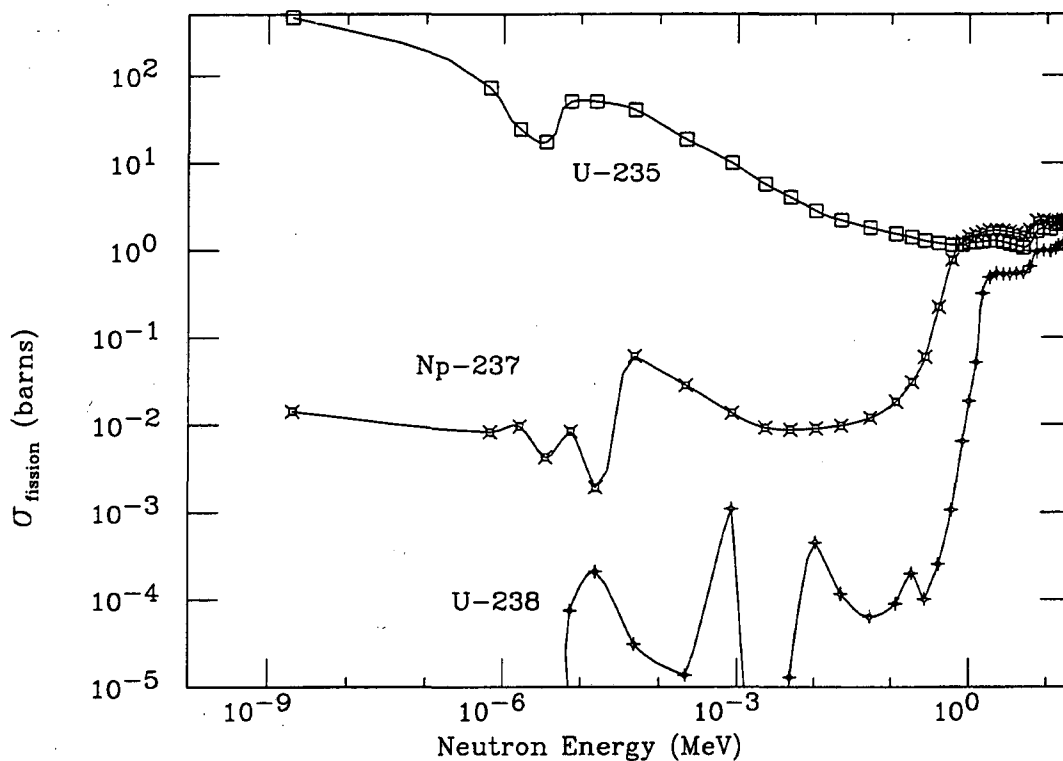
Figure 3.3: Fission cross-sections vs. neutron energy for various isotopes plotted using the 37 energy group structure of FLUKA92.

The fission cross-sections for [238]U, [237]Np and [235]U [21] are shown in Fig. 3.3 and indicate the importance of neutrons with energies as low as 1-2 MeV even for depleted uranium targets. Second, the only single code known to us which may properly include production processes for neutron energies below 20 MeV is the CINDER90 code [22], which is not yet available for general use.

The design of enhanced fissioning targets in which moderators and reflectors surround the target to thermalize neutrons and take advantage of the large fission cross-sections for [235]U for low energies is tantalizing. The neutron fluence in a bare [235]UC target and for a moderated/reflected target as determined by the FLUKA tracklength estimator is shown in Fig. 3.4. Gains in fission product RNB intensities by the use of enhanced fission targets are still being investigated.

The results of several independent calculations of isotope yields which may be important for the determination of DOE nuclear facility categorization [18] are shown in Table 3.1, and includes the DOE Category threshold activity, 'ORIHET' estimates [23],
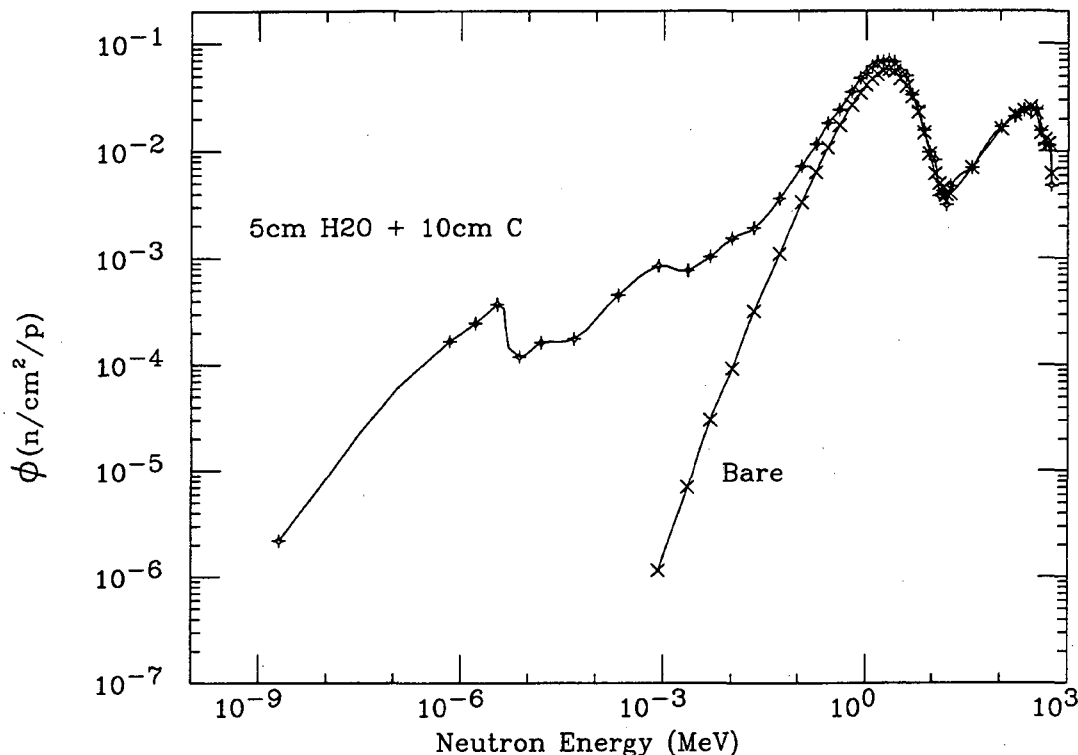
Figure 3.4: Target neutron fluence for a bare and moderated/reflected uranium carbide (^{235}U) target using the FLUKA tracklength estimator. The moderated/reflected case surrounds the target with 5 cm water followed by 10 cm graphite, respectively. Fluence has been normalized by the log of the energy bin width.

LAHET calculations and Tsao and Silberberg calculations.The results assume a 100 μA, 600 MeV proton beam incident on a 1 mole/cm^2 ($\sim$20 cm long) ^{235}UC target and 7 days of irradiation. Growth and decay calculations are included. 'ORIHET' gives an estimate using results from the 30 kg ^{238}U ISIS spallation source target at Rutherford Appleton Laboratory scaled to the relative energy deposition in our $\sim$1 kg target. This model is based on the HETC/ORIHET model developed by Atchison [24].

LAHET calculations give the spallation and fast fission yields above 20 MeV. In general, spallation product yields from LAHET and TSAO, such as ^{210}Po or ^{123}Sn, agree within a factor of 2 to 3 with ORIHET, whereas a comparison of fission product yields vary by factors of 2 to 10. This may be due to the additional fissions below 20 MeV and/or the normalization of the ORIHET estimates to our target. Comparison between TSAO and LAHET is surprisingly good since LAHET yields do not include contributions made

Table 3.1: Radioactive inventory assuming a 100 μA, 600 MeV proton beam on 1 mole/cm^2 UC target and 7 days irradiation.

Nuclide	$T_{\frac{1}{2}}$	DOE Cat3 (Ci)	ORIHET ^{238}U (Ci)	TSAO ^{235}UC (Ci)	LCS ^{235}UC (Ci)
^{131}I	8.04 d	0.92	650.00	81.5	51.1
^{125}I	60.14 d	0.56	13.00	5.9	4.6
^{140}Ba	12.75 d	600.00	680.00	53.8	22.1
^{99}Mo	65.94 h	3400.00	2300.00	248.0	156.7
^{91}Y	58.51 d	360.00	120.00	24.6	15.0
^{210}Po	138.38 d	1.90	0.63	0.68	0.22
^{89}Sr	50.53 d	340.00	93.00	27.3	16.8
^{95}Zr	64.02 d	700.00	180.00	17.9	12.2
^{144}Ce	284.89 d	100.00	25.00	2.0	0.89
^{106}Ru	373.59 d	100.00	17.00	3.2	2.0
^{129}Te	33.6 d	400.00	27.00	18.5	12.7
^{133}Xe	5.24 d	20000.00	940.00	112.9	75.0
^{90}Sr	29.1 y	16.00	0.59	0.13	0.08
^{123}Sn	129.2 d	320.00	10.00	4.1	4.2
^{137}Cs	30.1 y	60.00	1.00	0.08	0.04

by neutron reactions below 20 MeV. It should be noted that the predicted yields of the fission product ^{131}I firmly establishes ISL as a Category 3 nuclear facility.

Table 3.2: Radioactive inventory assuming a 100 μA, 600 MeV proton beam on 1 mole/cm^2 UC, La, Ta, and Pb targets and 7 days irradiation.

Nuclide	DOE Cat3 Threshold (Ci)	TSAO ^{235}UC (Ci)	TSAO Pb (Ci)	TSAO Ta (Ci)	TSAO La (Ci)
^{131}I	0.92	81.5	0.008	0.0001	0.25
^{125}I	0.56	5.9	0.19	0.155	20.1
^{140}Ba	600.00	53.8	0.003	0.0002	-
^{99}Mo	3400.00	248.0	3.1	0.276	0.06
^{91}Y	360.00	24.6	0.63	0.047	0.008
^{89}Sr	340.00	27.3	0.43	0.039	0.004
^{95}Zr	700.00	17.9	0.11	0.014	0.007
^{144}Ce	100.00	2.0	3.5×10^{-5}	7.4×10^{-5}	-
^{106}Ru	100.00	3.2	0.008	0.0011	0.0008
^{129}Te	400.00	18.5	0.043	0.0001	0.03
^{133}Xe	20000.00	112.9	0.016	0.0005	1.7
^{90}Sr	16.00	0.13	0.001	0.0001	1.1×10^{-5}
^{123}Sn	320.00	4.1	0.003	0.0004	0.002
^{137}Cs	60.00	0.08	1.2×10^{-6}	4.2×10^{-8}	0.0009

A comparison of the isotopic yields of different high-Z targets using the TSAO model is shown in Table 3.2. The results include corrections for buildup and decay. The relative contributions of spallation yields and fission yields can be easily seen in Table 3.2.

For example, ^{131}I is the major contributor to the nuclear facility categorization 3 for the UC target. It is an abundant fission product on the neutron rich side of the valley of β-stability. ^{125}I is less abundant because it is on the proton rich side and is a shielded nucleus from β^- decay. For the lower Z targets fission is less prominent and therefore less ^{131}I is produced. However ^{125}I production via spallation becomes more prominent, particularly so for the La target. The UC and La targets produce ^{125}I over the DOE Category 3 activity limits by factors of ~90 and 36, respectively, while the Ta and Pb targets are lower than the thresholds by about a factor of 3. The uncertainties in these estimates may easily be factors of 2 to 3, and probably more for certain isotopes. The isotopes identified in Table 3.1 and Table 3.2 were isotopes which were above 10% of the DOE Category 3 threshold for the UC target only. Additional isotopes specific to each target, which may be above Category 3 limits, have not yet been identified.

The average time between target changes at the ISL has been assumed to be about 1 week. Targets will be stored for approximately 1 year before disposal. ^{125}I has a half-life of 60.14 days, and therefore an inventory of greater than three Ta or Pb targets would also establish the ISL as a DOE Category 3 nuclear facility.

Table 3.3: Hazardous waste limit concentrations and estimates of hazardous waste concentrations for various targets after 1 week irradiation with 1 GeV 100 μA protons and no cooling time. 40CFR limits are based on concentrations found in a leachate solution (see text).

| Element	40CFR Limit (ppm)	TSAO-UC (ppm)	TSAO-Pb (ppm)	TSAO-La (ppm)
Arsenic	5	4.1	2.5	0.25
Barium	100	34.6	0.37	172.8
Cadmium	1	71.2	21.8	16.8
Chromium	5	13.9	1.7	0.17
Lead	5	6.9	-	-
Mercury	0.2	11.9	167.0	-
Selenium	1	11.8	7.0	0.65
Silver	5	25.0	8.6	4.5

Table 3.3 shows the Toxicity Characteristic Leachate Procedure (TCLP) limits for elemental metals as taken from the Code of Federal Regulations [25], as well as estimates of these elements using the TSAO program for UC, Pb, and La targets. The TCLP test involves taking a 100 g sample which has been reduced to a size such that the pieces will pass through a 9.5 mm sieve, and placing it for about 24 hrs in a 2 liter solution of pH 3-5 acetic acid. The concentration found in the leachate solution is then compared with the 40CFR limits shown in Table 3.3. If the concentrations are in excess of these limits the material is defined as hazardous waste. If the material is also radioactive it is defined as mixed-waste. The TSAO estimates in Table 3.3 are the concentrations predicted *in the target*, not in the leachate solution. Determining the concentrations of various target products in the leachate solution would involve detailed solubility measurements or calculations which have not been made here. However, one can make several preliminary conclusions: the UC target exceeds the limits, but UC is very insoluble and is not likely to fail the TCLP test (*i.e.*, become mixed-waste), a powdered La target would probably completely dissolve resulting in concentrations which would be within a factor of 3 of the TCLP limits. The uncertainty of these calculations is at least of this order, resulting in a preliminary classification of a spent La target as mixed-waste. Lead itself is a hazardous substance making a spent Pb target also mixed-waste. Disposal of highly radioactive mixed-waste is difficult, if not impossible. The ISL community will have to work together with the DOE to provide a solution for permanent storage of spent targets, especially if further detailed calculations support the preliminary classification of mixed-waste.

4. Target Heating

The 100 μA, 600 MeV proton beam will deposit about 2/3rds of its energy non-uniformly in a high-Z target whose thickness is about 1 mole/cm^2. ISL target temperature profiles must be kept uniform to prevent products from condensing in cold pockets thus preventing their release from the target. Targets will be heated or cooled to achieve a uniform temperature profile.

This requires detailed estimates of 3-dimensional power density profiles. A comparison of the various energy deposition profiles as calculated with LAHET and FLUKA for a UC
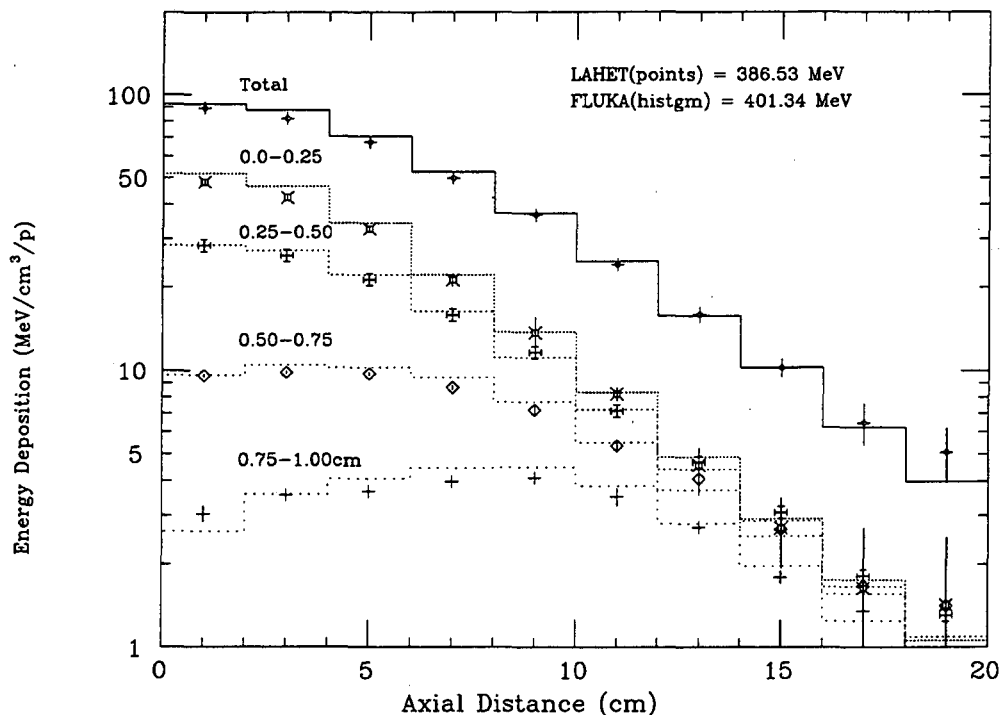
Figure 4.1: Energy deposition predictions in various radial bins by LA-HET (points) and FLUKA (histograms) for 600 MeV protons incident on a 20 cm long uranium carbide target.

(100% ^{235}U) bare target is shown in Fig. 4.1. The agreement between LAHET and FLUKA calculations is quite good for all radial intervals. Total energy deposition agrees within 1.2%. Comparisons of experimental data [26-27] with LAHET predictions [28] generally show good agreement for lead and bismuth with larger discrepencies for the low-Z targets, in particular the beryllium target. This will introduce some uncertainty in the performance of low-Z ISL targets.

An example of a 3-dimensional thermal stress analysis with ANSYS [29], using results from FLUKA86† [30] is shown in Fig. 4.2. In this figure, the target is represented as the 4 inner concentric cylinders with heat transfer fins on the outside. The entire assembly fits

---

$\dagger$ This version of FLUKA did not include fission energy deposition.

TEMPERATURES

■ 373 K
▨ 1200 K
■ 2000 K
▨ 2600 K
□ 3027 K
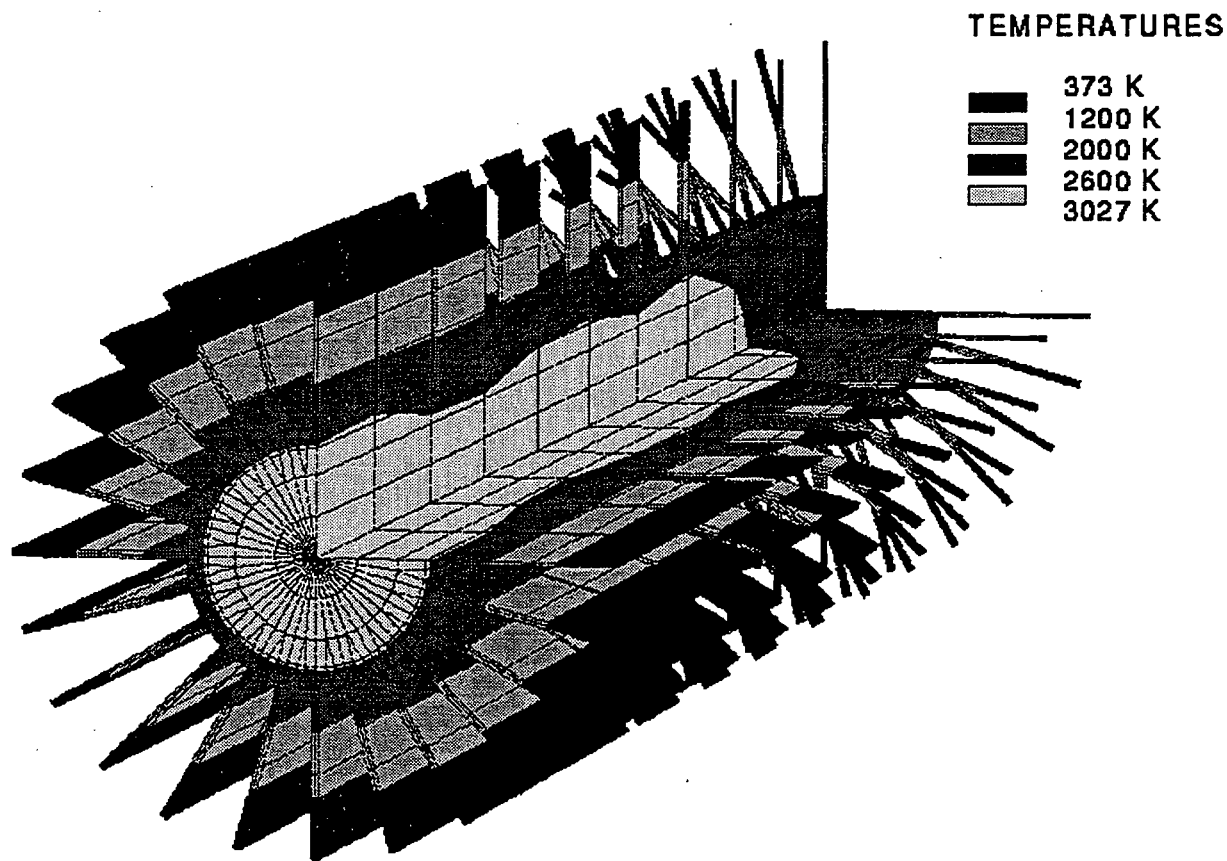
Figure 4.2: ANSYS analysis of thermal stress in a 20 cm long by 2 cm diameter ISL tantalum target with special heat fin design using FLUKA86 power density estimates. A 61 μA 800 MeV proton beam (σ=3 mm) is assumed to be incident on the front face of the target.

within a water cooled outer fixture. Temperature profiles may be kept uniform (within $\pm 10\%$) over the volume of the target by varying the thermal conductivity of the fins (widths of fins) along the length of the target. Investigations are under way to examine the possibility of He gas cooling of ISL targets.

5. Conclusions

Coupled Monte Carlo analyses and discrete ordinates analyses of shielding requirements of an ISL target in the lateral direction agree well with published simple models for thicknesses greater than about 40 cm [10]. Shielding in the forward direction is complicated by the relatively large number of cascade neutrons in thin shields. Simple models could be developed for medium-energy proton machines (0.2 - few GeV) to provide shielding estimates in the forward direction. However, such simple models would probably not be valid for thicknesses less than approximately 1 m. Monte Carlo analyses would still be needed for problems such as radiation damage estimates close to the targets.

Detailed estimates of induced activity produced in the targets are essential for at least three reasons: First, the ISL must provide researchers with estimates of RNB's that can be delivered to experimental stations. These intensities depend on many factors, such as ionization and acceleration efficiencies, but are ultimately based on target yields. Second, the classification of the ISL (or any high-intensity, medium proton energy facility) as a "non-reactor, nuclear facility" depends strictly on the inventory of radioactivity. Third, targets to be discarded must be characterized. This characterization also involves estimates of the concentration of hazardous materials produced in the targets. Targets characterized as mixed-waste would be very difficult and expensive to discard. To date, no single tool has been found to provide such estimates for the wide variety of ISL targets. Models should be developed which can provide low-energy fission mass yields as well as the higher-energy spallation/fission/fragmentation mass yields. For those programs that do provide estimates from spallation/fast fission, little exists in the way of experimental verification.

Estimates of energy deposition in ISL targets using two independent codes have been made and agreement between codes is very good. There may have been earlier discrepencies due to the treatment (or lack of treatment) of certain processes, like fission, but they seem to have been eliminated. Comparisons with experimental data show some discrepencies, particularly for low-Z targets [28].

Acknowledgements

References

1. *Proceedings of The First International Conference on Radioactive Nuclear Beams,* Berkeley, 1989, edited by W. D. Meyer, J. M. Nitschke, and E. B. Norman (World Scientific, Singapore, 1990).

2. *Proceedings of The Workshop on the Science of Intense Radioactive Ion Beams,* edited by J. B. McClelland and D. J. Vieira, Los Alamos, NM. , 1990.

3. *Proceedings of The International Workshop on the Physics and Techniques of Secondary Nuclear Beams,* edited by J. F. Bruandet, B. Fernandez, and M. Bex, Dourdan, France, 1992.

4. *Proceedings of The Second International Conference on Radioactive Nuclear Beams,* edited by T. Delbar, Louvain-la-Neuve, 1991.

5. *Proceedings of The Workshop on the Production and Use of Intense Radioactive Beams at the IsoSpin Laboratory,* edited by J. G. Garrett, Oak Ridge, TN, 1992.

6. J. M. Nitschke, *Accelerated Radioactive Nuclear Beams: Existing and Planned Facilities,* Proceedings of the 13th International Conference on Cyclotrons and Their Applications, edited by G. Dutto and M. K. Craddock (Vancouver, Canada, 1992) p. 713.

7. *The IsoSpin Laboratory: Research Opportunities with Radioactive Nuclear Beams,* LALP 91-51 (1991).

8. *European Radioactive Beam Facilities,* NuPECC Report, May (1993).

9. J. M. Nitschke, *Future Prospects for Radioactive Nuclear Beams in North America,* Proceedings of The International School Seminar on Heavy Ion Physics (Dubna, Russia, 1993) p. 1374.

10. K. Tesch, *A Simple Estimation of the Lateral Shielding for Proton Accelerators in the Energy Range 50 to 1000 MeV*, Radiation Protection Dosimetry **11** (3), 165 (1985).

11. R. E. Prael and H. Lichtenstein, *User Guide to LCS: The LAHET Code System*, Los Alamos National Laboratory Report LA-UR-89-3014 (1989).

12. R. D. O'Dell, *et al.*, *Revised User's Manual for ONEDANT: A Code Package for One Dimensional, Diffusion Accelerated, Neutral Particle Transport*, Los Alamos National Laboratory Report LA-9184-M (1989).

13. R. G. Alsmiller Jr., J. M. Barnes and J. D. Drischler, *Neutron-Photon Multigroup Cross Sections for Neutron Energies ≤400 MeV (Revision 1)*, NIM **A249**, 455-460 (1986).

14. *Review of Particle Properties*, Phys. Rev. D**45** 2 (1992).

15. Belogorev, *et al.*, *Depth Dose and Depth Dose Equivalent Data for Beutrons with Energy from Thermal up to Several TeV*, NIM **199** (1982) 563-572.

16. *ISOLDE Users' Guide*, edited by H. J. Kluge, CERN 86-05.

17. J. Domingo *et al.*, *Design Study of the Proposed SIN-ISOLDE Facility*, NIM **186**, 79-86 (1981).

18. DOE Standard *Hazard Categorization and Accident Analysis Techniques for Compliance with DOE Order 5480.23, Nuclear Safety Analysis Reports*, DOE-STD-1027-92 (1992).

19. R. Silberberg and C. H. Tsao, The Astrophysical Journal Supplement Series **58**, 873 (1985).

20. A. Fassò *et al.*, *FLUKA92*, presented at the Workshop on Simulating Accelerator Radiation Environments, Santa Fe, NM (1993).

21. A. Ferrari, INFN (private communication).

22. W. B. Wilson, *et al.*, *Accelerator Transmutation Studies at Los Alamos with LAHET, MCNP, and CINDER'90*, presented at the Workshop on Simulating Accelerator Radiation Environments, Santa Fe, NM (1993).

23. T. Broome, Rutherford Appleton Laboratory, UK (private communication).

24. F. Atchison, *A Theoretical Study of a Target Reflector and Moderator Assembly for SNS*, RL-81-006, Rutherford and Appleton Laboratories (1981).

25. *U. S. Environmental Protection Agency Regulations on Hazardous Waste Characteristics, Code of Federal Regulations*, Section 261.20 (1992).

26. V. I. Belyakov-Bodin *et al.*, *Calorimetric Measurements and Monte Carlo Analyses of Medium-Energy Protons Bombarding Lead and Bismuth Targets*, NIM **A295** (1990) 140-146.

27. V. I. Belyakov-Bodin *et al.*, *Calorimetric Measurements of Medium-Energy Protons Bombarding Beryllium, Carbon and Aluminum Targets*, NIM **A314** (1992) 508-513.

28. C. A. Beard *et al.*, *Comparison of Energy Deposition Calculations by the LAHET Code System with Experimental Results for 800, 1000, and 1200 MeV Protons on Lead, Bismuth, Beryllium, Carbon and Aluminum*, LA-UR-93-541, Los Alamos National Laboratory, Los Alamos, NM.

29. G. J. De Salvo and R. W. Gorman, *ANSYS Engineering Analysis System*, Swanson Analysis Systems, Inc. , Houston, PA. ,Version 4.4 (1989).

30. T. W. Eaton, H. L. Ravn and the ISOLDE Collaboration, *Beam Heating of Thick Targets for On-Line Mass Separators*, NIM **B26**, 190 (1987).